

HOPFORMER: SPARSE GRAPH TRANSFORMERS WITH EXPLICIT RECEPTIVE FIELD CONTROL

PREPRINT

Sanggeon Yun, Raheeb Hassan, Ryozo Masukawa, Sungheon Jeong, and Mohsen Imani

Department of Computer Science, University of California, Irvine
 {sanggeoy, raheebh, rmasukaw, sungheoj, m.imani}@uci.edu

ABSTRACT

Graph Transformers typically rely on explicit positional or structural encodings and dense global attention to incorporate graph topology. In this work, we show that neither is essential. We introduce HopFormer, a graph Transformer that injects structure exclusively through head-specific n -hop masked sparse attention, without the use of positional encodings or architectural modifications. This design provides explicit and interpretable control over receptive fields while enabling genuinely sparse attention whose computational cost scales linearly with mask sparsity. Through extensive experiments on both node-level and graph-level benchmarks, we demonstrate that our approach achieves competitive or superior performance across diverse graph structures. Our results further reveal that dense global attention is often unnecessary: on graphs with strong small-world properties, localized attention yields more stable and consistently high performance, while on graphs with weaker small-world effects, global attention offers diminishing returns. Together, these findings challenge prevailing assumptions in graph Transformer design and highlight sparsity-controlled attention as a principled and efficient alternative.

1 INTRODUCTION

Transformers [11] have become a dominant architecture in modern machine learning due to their expressive self-attention mechanism and strong scalability with respect to data and model size. By relying on weak inductive biases, Transformers learn task-relevant structure directly from data, a property that has driven their success in domains characterized by long-range dependencies and heterogeneous interactions, including natural language processing [12] and vision [13].

Extending Transformers to graph-structured data has therefore attracted growing interest as an alternative to Message-Passing Graph Neural Networks (MPNNs) [14]. While MPNNs leverage sparse local aggregation and achieve strong empirical performance, their strictly local propagation limits the ability to capture long-range dependencies and global structural patterns, leading to phenomena such as over-smoothing [15] and information bottlenecks in deep architectures [16]. These limitations have motivated the adoption of Transformer-style attention to enable broader interaction ranges on graphs.

Applying Transformers to graphs, however, is fundamentally more complex than in sequential domains. Graphs are non-sequential, permutation-invariant structures [17] with heterogeneous information sources, including node attributes, edge attributes, and relational topology [18]. As a result, most existing graph Transformer models modify the standard Transformer design to explicitly inject structural information. Common strategies include adding positional or structural encodings—such as shortest-path distances, centrality measures, Laplacian eigenvectors, diffusion kernels, or random-walk statistics—into attention logits or node embeddings [19, 1, 2, 3, 9]. Other approaches introduce architectural modifications, such as hybrid message-passing and attention blocks or auxiliary structural tokens [3, 9, 5, 7, 10]. A systematic comparison of these design choices is summarized in Table 1.

Despite their strong empirical performance, these developments raise fundamental questions about the necessity of prevailing graph Transformer design choices. First, **is it truly necessary to inject graph structure through explicit positional or structural encodings, or through architectural modifications of the Transformer itself?** Such encodings are highly sensitive to their formulation, dimensionality, scaling, and point of integration [20, 21, 22], and they can impair generalization when test-time graph sizes or structural distributions differ from those observed during training [22]. In contrast, recent results in sequence modeling demonstrate that Transformers can recover both absolute and relative positional information using attention masking alone, even without explicit positional embeddings [20, 23, 22]. These findings suggest that structural inductive bias may be imposed implicitly through constrained attention patterns, without relying on handcrafted encodings or auxiliary architectural components.

Second, **is dense global self-attention essential for effective graph representation learning?** Although many graph Transformers retain global attention over all token pairs, real-world graphs frequently exhibit strong small-world properties [24, 25], where informative interactions are concentrated within a limited number of hops. Moreover, global attention incurs quadratic or worse computational cost. When both nodes V and edges E are treated as tokens—a common strategy for modeling heterogeneous graph information [1, 5]—the attention matrix scales as $(|V| + |E|) \times (|V| + |E|)$, leading to prohibitive $O(|V|^4)$ complexity in dense graphs. This raises the question of whether dense global attention is necessary at all, or whether carefully structured, locality-aware attention mechanisms can suffice to capture both local and long-range dependencies.

To answer these questions, we propose HopFormer, a new graph Transformer paradigm that adopts the simplest design principles proven effective in sequential Transformer models. Our ap-

Table 1: Comparison of graph learning architectures by core design components. \checkmark indicates preservation of the vanilla Transformer architecture (i.e., standard multi-head self-attention and feed-forward blocks without architectural modifications), while \times denotes architectural modifications. Here, $|V|$ and $|E|$ denote the number of nodes and edges in the input graph, respectively. “Flexible” complexity indicates that the computational cost adapts to graph sparsity and head-specific receptive fields, scaling at least linearly with $|V| + |E|$ under sparse attention, rather than incurring dense quadratic cost.

Method	Structural / Positional Encoding	Vanilla Transformer	Attention Pattern	Complexity per Layer
MPNNs	–	–	Sparse (local)	$O(E)$
Graphomer [1]	SPD, centrality	\times	Dense Global Attention	$O(V ^2)$
SAN [2]	Laplacian eigenvectors	\times	Dense Global Attention	$O(V ^2)$
GraphGPS [3]	Structural encodings	\times	Dense Global Attention	$O(V ^2)$
NodeFormer [4]	Random features	\times	Approximated Global Attention	$O(V + E)$
TokenGT [5]	Structural / edge encodings	\checkmark	Dense Global Attention	$O((V + E)^2)$
SpecFormer [6]	Spectral features	\times	Dense Global Attention	$O(V ^2)$
DIFFomer [7]	Diffusion kernels	\times	Dense Global Attention	$O(V ^2)$
Exphormer [8]	Subgraph encodings	\times	Sparse Attention	$O(E)$
GRIT [9]	Learned structural tokens	\times	Dense Global Attention	$O(V ^2)$
ESA [10]	None	\times	Masked+Dense Global Attention	$O(E ^2)$
Ours (HopFormer)	None	\checkmark	Sparse Attention Guided by n-Hop Masks	Flexible with $\Omega(V + E)$

proach injects graph structure exclusively through *head-specific n -hop masked sparse attention*, in which each attention head is restricted to a prescribed n -hop receptive field via attention masks, without relying on positional or structural encodings and without modifying the standard Transformer architecture. Importantly, these masks are applied *prior* to attention computation, so self-attention is performed only on the masked support, yielding genuinely sparse attention rather than masked dense attention. By explicitly controlling the hop radius per head, our design exposes a direct and interpretable trade-off between receptive field size and computational cost. To jointly model node and edge information without auxiliary encodings, we employ a node–edge tokenization scheme based on an augmented incidence graph, treating edges as auxiliary tokens connected to their endpoints. Node and edge attributes are embedded using lightweight, modality-specific input projections into a shared latent space, following established practice in multimodal Transformers [26, 27]. This formulation enables unified attention over heterogeneous graph components while preserving architectural simplicity.

Our theoretical analysis and extensive experiments demonstrate that explicit positional or structural encodings are not a prerequisite for effective graph Transformers. Instead, we show that graph structure can be fully and efficiently injected through head-specific n -hop masked sparse attention alone, without modifying the standard Transformer architecture. Moreover, our results reveal that dense global attention is often unnecessary: on graphs with strong small-world properties, carefully controlled local receptive fields not only suffice but yield more stable and consistently strong performance across datasets. Even on graphs with weaker small-world effects, global attention exhibits diminishing returns, with multiple Transformer variants converging to similar performance. Together, these findings establish that explicit, topology-aligned control of attention sparsity offers a principled and generalizable alternative to increasingly complex graph Transformer designs, achieving competitive accuracy with improved interpretability and computational efficiency.

2 RELATED WORK AND BACKGROUND

Attention Masking and Structural Bias. Attention masking provides a principled mechanism for constraining information flow in Transformers without altering the attention operator itself. In sequence models, causal masking has been shown to implicitly induce positional structure, allowing Transformers to recover absolute and relative positional relationships even without explicit positional embeddings [20, 23, 22]. Motivated by these findings, we adopt masking as the sole mechanism for injecting structural inductive bias in graph Transformers. Specifically, we employ head-specific n -hop attention masks that bound each attention head’s receptive field according to graph topology, providing explicit and interpretable control over information propagation while preserving the standard self-attention formulation.

Sparse Attention and Sparse Computation. Sparse matrix operations enable efficient computation when interactions are inherently sparse, with time complexity proportional to the number of nonzero entries, i.e., $O(\text{nnz})$, rather than quadratic in problem size [28]. In graph learning, MPNNs naturally leverage sparsity by formulating neighborhood aggregation as sparse matrix operations [14, 29]. However, many graph Transformers retain dense global self-attention over all K tokens, incurring $O(K^2)$ complexity regardless of graph sparsity. Even when attention masks are employed, dense attention scores are often computed prior to masking, resulting in masked dense attention rather than true sparsity. In contrast, our approach applies masks *before* attention computation, enabling attention to be implemented directly via sparse operations with complexity scaling as $O(\text{nnz}(\mathbf{M}))$, where \mathbf{M} denotes the attention mask.

Small-World Property. Given a graph $G = (V, E)$, where $d(u, v)$ denotes the shortest-path distance between nodes $u, v \in V$, many real-world graphs exhibit the *small-world* property, characterized by a small average shortest-path length

$$\ell(G) = \frac{1}{|V|(|V| - 1)} \sum_{u \neq v} d(u, v) = O(\log |V|), \quad (1)$$

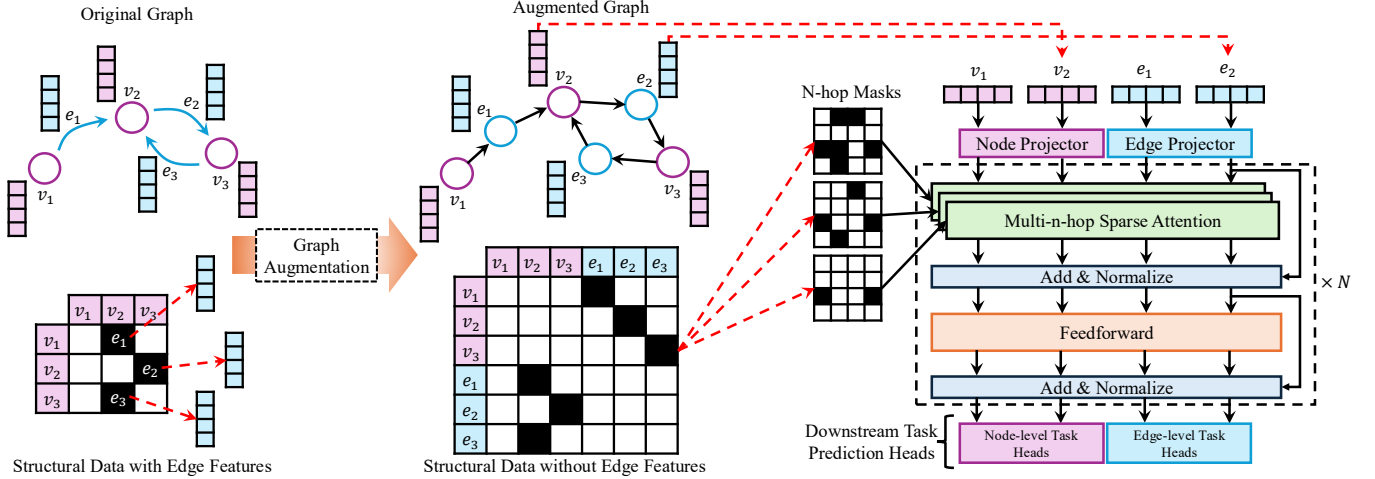


Figure 1: An illustration of the proposed edge-to-node augmentation, node–edge tokenization, and head-specific n -hop sparse attention mechanism.

together with a high clustering coefficient

$$C(G) = \frac{1}{|V|} \sum_{v \in V} \frac{2|\mathcal{N}(v)|}{\deg(v)(\deg(v) - 1)}, \quad (2)$$

where $\mathcal{N}(v)$ denotes the set of edges between neighbors of v and $\deg(v)$ is the degree of v . Such properties are widely observed in social, biological, and information networks [24, 25]. They imply that informative interactions are typically concentrated within a small number of hops, rendering dense global attention unnecessary at every layer and motivating attention mechanisms that explicitly restrict receptive fields while retaining the ability to capture long-range dependencies.

3 METHODOLOGY

In this section, we introduce HopFormer, a graph Transformer that injects structure solely through head-specific attention masks while leaving the standard Transformer architecture intact (Figure 1). Our design enables explicit control over attention receptive fields, avoiding redundant global interactions on small-world graphs, and preserves sparse attention computation for improved efficiency—without relying on positional or structural encodings.

3.1 Edge-to-Node Augmentation via Incidence Graph

Let $G = (V, E)$ be a graph with $|V| = N$ nodes and $|E| = M$ edges. Each node $v \in V$ is associated with a feature vector $\mathbf{x}_v \in \mathbb{R}^{d_v}$, and each edge $e \in E$ may optionally carry features $\mathbf{e}_e \in \mathbb{R}^{d_e}$. To enable a unified treatment of nodes and edges as tokens in a Transformer, we first convert G into an *augmented incidence graph* $\tilde{G} = (\tilde{V}, \tilde{E})$ by converting each edge into an *edge node*. Concretely, let $\tilde{V} = V \cup E$ where we identify each $e = (u, v) \in E$ with a new vertex also denoted e . We then connect each edge-node to its endpoint nodes:

$$\tilde{E} = \{(u, e), (e, u), (v, e), (e, v) \mid e = (u, v) \in E\}. \quad (3)$$

Thus each original edge becomes two undirected incidence links (or four directed links), and the augmented graph has $|\tilde{V}| = N+M$ and $|\tilde{E}| = \Theta(M)$. Importantly, this transformation preserves sparsity up to a constant factor and does not alter the asymptotic edge complexity of the original graph.

3.2 Input Projectors for Node–Edge Tokenization

Based on the augmented incidence graph \tilde{G} , we represent the augmented node set \tilde{V} as a collection of tokens consisting of node tokens, corresponding to $V \cap \tilde{V}$, and edge tokens, corresponding to $E \cap \tilde{V}$. To accommodate heterogeneous feature spaces without modifying the Transformer layers, we employ lightweight *input projectors* to map node and edge attributes into a shared d -dimensional token space:

$$\mathbf{h}_v = \mathbf{W}_n \mathbf{x}_v, \quad v \in V \cap \tilde{V}, \quad \mathbf{h}_e = \mathbf{W}_e \mathbf{e}_e, \quad e \in E \cap \tilde{V}, \quad (4)$$

with $\mathbf{W}_n \in \mathbb{R}^{d \times d_v}$ and $\mathbf{W}_e \in \mathbb{R}^{d \times d_e}$. If edge features are unavailable, we set $\mathbf{e}_e = \mathbf{0}$ so that edge tokens contribute only through topology. The resulting input token sequence is

$$\mathbf{H}^{(0)} = [\{\mathbf{h}_v\}_{v \in V \cap \tilde{V}}; \{\mathbf{h}_e\}_{e \in E \cap \tilde{V}}] \in \mathbb{R}^{(N+M) \times d}. \quad (5)$$

This construction treats nodes and edges symmetrically as tokens and avoids auxiliary modules (e.g., cross-attention) or separate update rules.

3.3 Head-Specific n -Hop Sparse Attention

We inject graph structure into the Transformer exclusively through *head-specific attention masks* derived from the augmented incidence graph \tilde{G} . These masks depend only on the connectivity encoded by \tilde{E} and do not incorporate edge attributes or any additional structural features, leaving all other components of the Transformer architecture unchanged.

Let $\tilde{\mathbf{A}} \in \{0, 1\}^{(N+M) \times (N+M)}$ denote the sparse adjacency matrix of \tilde{G} . For each attention head $h \in \{1, \dots, H\}$, we assign a hop

budget $n_h \in \mathbb{N}$, which defines the maximum receptive field of that head in terms of graph distance.

Conceptually, we define the head-specific attention mask as the n_h -hop reachability matrix

$$\mathbf{M}^{(h)} = \mathbb{I} \left[\sum_{k=0}^{n_h} \widetilde{\mathbf{A}}^k > 0 \right] \in \{0, 1\}^{(N+M) \times (N+M)}, \quad (6)$$

where $\widetilde{\mathbf{A}}^0 = \mathbf{I}$ and the indicator function is applied elementwise. An entry $\mathbf{M}_{ij}^{(h)} = 1$ indicates that token j is reachable from token i within at most n_h incidence hops in \widetilde{G} .

Given token embeddings $\mathbf{H} \in \mathbb{R}^{(N+M) \times d}$, attention head h computes scaled dot-product attention restricted to the support of $\mathbf{M}^{(h)}$:

$$\text{Attn}^{(h)}(\mathbf{Q}, \mathbf{K}, \mathbf{V}) = \text{softmax} \left(\frac{(\mathbf{Q}\mathbf{K}^\top)_{\mathbf{M}^{(h)}}}{\sqrt{d_h}} \right) \mathbf{V}, \quad (7)$$

where $d_h = d/H$ and $(\cdot)_{\mathbf{M}^{(h)}}$ denotes restriction to the nonzero entries specified by the mask. Equivalently, attention scores are computed *only* for token pairs whose graph distance is at most n_h , while all other interactions are excluded from both computation and normalization.

Sparse attention implementation. Because attention is restricted *prior* to score computation, the resulting operation constitutes genuine sparse attention rather than masked dense attention. The number of attention interactions per head is determined by the size of the n_h -hop neighborhoods in \widetilde{G} and therefore depends on graph topology and hop budget, rather than on the total number of tokens ($N + M$). This allows attention to be implemented directly over sparse supports, with computational cost proportional to $\text{nnz}(\mathbf{M}^{(h)}) \cdot d_h$. Consequently, each head explicitly trades receptive field size for computational cost through its hop budget n_h , yielding interpretable and topology-aligned control over attention.

3.4 Overall Transformer Architecture

Our model follows the standard Transformer encoder architecture [11] without modifying its layer structure, residual connections, normalization, or feed-forward networks. Graph structure is injected *exclusively* through the multi-head self-attention module by replacing dense global attention with head-specific masked attention, while all other components remain identical to the vanilla Transformer.

Let $\mathbf{Z}^{(\ell)} \in \mathbb{R}^{T \times d}$ denote the token representations at layer ℓ , where $T = N + M$. Each layer is defined as

$$\widetilde{\mathbf{Z}}^{(\ell)} = \underbrace{\text{MHSA}_{\{\mathbf{M}^{(h)}\}_{h=1}^H}(\mathbf{Z}^{(\ell)})}_{\text{only difference from vanilla Transformer}} + \mathbf{Z}^{(\ell)}, \quad (8)$$

$$\mathbf{Z}^{(\ell+1)} = \text{FFN}(\widetilde{\mathbf{Z}}^{(\ell)}) + \widetilde{\mathbf{Z}}^{(\ell)}. \quad (9)$$

Here, $\text{MHSA}_{\{\mathbf{M}^{(h)}\}_{h=1}^H}$ denotes masked multi-head self-attention, in which each head h computes attention using the head-specific n_h -hop mask $\mathbf{M}^{(h)}$ via the masked attention operator defined in Equation 7. Apart from the inclusion of these masks, the attention computation and head aggregation are identical to those in the standard Transformer [11].

3.5 Training with Downstream Tasks

Let $\{\mathbf{h}_v^{(L)}\} = \mathbf{H}^{(L)} \in \mathbb{R}^{(N+M) \times d}$ denote the output token representations from the final Transformer layer. For node-level tasks, predictions are obtained by applying a shared classifier f_{node} to node tokens:

$$\hat{\mathbf{y}}_v = f_{\text{node}}(\mathbf{h}_v^{(L)}), \quad v \in V \cap \widetilde{V}, \quad (10)$$

and the model is trained using standard node-wise losses, such as cross-entropy for classification.

For graph-level tasks, a permutation-invariant readout function $\rho(\cdot)$ aggregates token representations into a single graph representation:

$$\mathbf{h}_G = \rho(\{\mathbf{h}_v^{(L)}\}_{v \in V \cap \widetilde{V}} \cup \{\mathbf{h}_e^{(L)}\}_{e \in E \cap \widetilde{V}}), \quad (11)$$

which is then mapped to the prediction $\hat{\mathbf{y}}_G = f_{\text{graph}}(\mathbf{h}_G)$ using a task-specific head. Typical choices for ρ include sum or mean pooling.

All parameters, including input projectors and Transformer layers, are optimized jointly via backpropagation by minimizing the downstream loss. Since graph structure is incorporated solely through head-specific attention masks, the training procedure is identical to that of a standard Transformer, while yielding topology-aware and sparsity-preserving representations.

4 THEORETICAL ANALYSIS

We provide a theoretical analysis of the proposed HopFormer to justify two central claims: (i) injecting graph structure solely through head-specific attention masks is sufficient to convey structural information to the Transformer, and (ii) equipping a single Transformer layer with multiple heads of different receptive fields strictly increases its expressiveness.

Assumption 1 (Full-rank projections). Following standard assumptions in expressiveness analyses of attention-based models (e.g., [30, 31]), we assume that the value projection matrices $\mathbf{W}_V^{(h)} \in \mathbb{R}^{d_h \times d}$ for all heads $h \in \{1, \dots, H\}$ are full rank, i.e.,

$$\text{rank}(\mathbf{W}_V^{(h)}) = d_h, \quad d_h = d/H. \quad (12)$$

This ensures that no information loss is introduced by linear value projections.

Assumption 2 (Injective post-attention mapping). Let $\phi(\cdot)$ denote the composition of the output projection, residual connection, and any subsequent nonlinearity (e.g., feed-forward network). We assume ϕ is injective:

$$\phi(\mathbf{z}_1) = \phi(\mathbf{z}_2) \Rightarrow \mathbf{z}_1 = \mathbf{z}_2. \quad (13)$$

This assumption is commonly adopted to isolate the expressive power of the attention mechanism itself [30].

Assumption 3 (Sparse topology and bounded hops). The augmented graph \widetilde{G} is sparse, with $|\widetilde{E}| = O(M)$, and hop budgets $\{n_h\}_{h=1}^H$ are bounded by a small constant independent of N and M .

Assumption 4 (Distinct receptive fields). There exist at least two heads $h \neq h'$ such that $n_h \neq n_{h'}$.

4.1 Sufficiency of Structural Information Injection via Masked Attention

We first show that attention masks derived from \tilde{G} alone are sufficient to inject graph structure into the Transformer layer.

Theorem 1 (Topology-Constrained Information Flow). *For an attention head h with hop budget n_h , the output representation of any token i after a single attention layer depends exclusively on tokens within the n_h -hop neighborhood of i in the augmented incidence graph \tilde{G} .*

(*Proof*: Appendix 8.1)

Corollary 1 (Sufficiency of Mask-Based Structure Injection). *Even without positional or structural encodings, the Transformer layer is explicitly graph-aware, as all information propagation is constrained by the topology of \tilde{G} encoded in the attention masks.*

4.2 Expressiveness of Multi- n -Hop Heads

We now establish that multiple heads with distinct hop budgets increase the expressive power of a single Transformer layer.

Theorem 2 (Strict Expressiveness Gain of Multi- n -Hop Heads). *Under Assumptions 1–4, a Transformer layer with multiple attention heads having distinct hop budgets $\{n_h\}_{h=1}^H$ is strictly more expressive than any layer in which all heads share a common hop budget.*

(*Proof*: Appendix 8.2)

Corollary 2 (Multi-Scale Representation in a Single Layer). *A single Transformer layer with heterogeneous hop budgets can simultaneously model local and longer-range dependencies, enabling multi-scale graph representations without increasing depth.*

Together, **Theorem 1** and its corollary demonstrate that head-specific attention masks alone are sufficient to inject graph structure into a Transformer layer. Furthermore, **Theorem 2** and its corollary establish that employing multiple heads with distinct hop budgets strictly enhances expressiveness by enabling multi-scale neighborhood aggregation within a single layer. Collectively, these results provide a principled justification for HopFormer as a sparse, topology-aware Transformer that attains increased expressive power without auxiliary encodings or architectural modifications beyond masked self-attention.

5 EXPERIMENTS

5.1 Experimental Setting

We follow the standardized and fully reproducible experimental protocols established in OpenGT [32], ensuring fair and consistent comparisons across models, datasets, and tasks.

Baselines. We compare against a comprehensive set of state-of-the-art Graph Transformer architectures, including DIFFormer [7], NodeFormer [4], GraphGPS [3], Graphormer [1], GRIT [9], SGFormer [33], SAN [2], SpecFormer [6], Exphormer [8], GraphTransformer [34], GraphMLPMixer [35], CoBFormer [36], and DeGTA [37]. In addition, we include

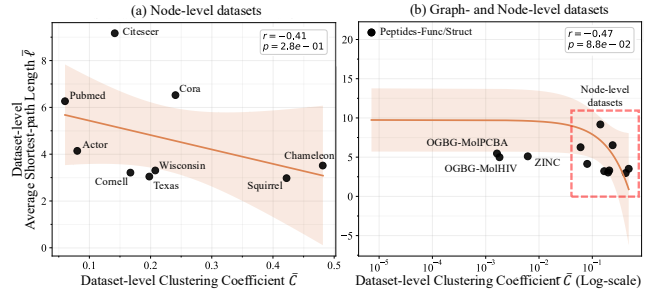


Figure 2: Small-world measures of (a) node-level and (b) graph- and node-level benchmark datasets. Graph-level datasets generally exhibit weaker small-world characteristics than node-level datasets. The shaded region denotes the standard deviation of the linear fit.

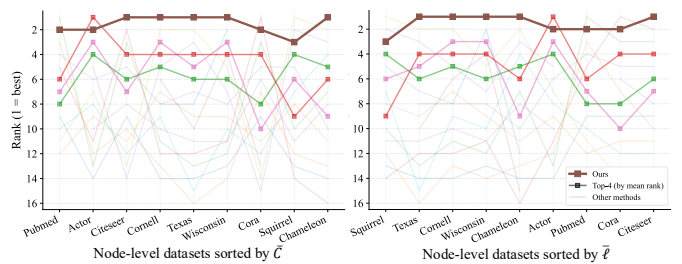


Figure 3: Rank trajectories of different methods across node-level datasets. Our method maintains consistently strong ranks, while other approaches exhibit larger variability as datasets’ small-world characteristics change.

representative message-passing GNNs—GCN [38], GAT [39], and APPNP [40]—to contrast Transformer-based models with local aggregation baselines.

Datasets. We evaluate on a diverse suite of node-level and graph-level benchmarks summarized in Appendix Table 4. Node-level tasks span citation networks (Cora, Citeseer, Pubmed [41]), web graphs (Chameleon, Squirrel [42]), actor co-occurrence graphs (Actor [43]), and heterophilous university web networks (Texas, Cornell, Wisconsin [44]). Graph-level tasks include molecular property prediction (ZINC [45], OGBG-MolHIV, OGBG-MolPCBA [46]) and peptide benchmarks from LRGB (Peptides-Func, Peptides-Struct [47]). These datasets exhibit wide variation in size, sparsity, homophily, and small-world characteristics, enabling a thorough evaluation across structural regimes.

Implementation and Hyperparameters. All baseline models are implemented using the OpenGT codebase [32]. For each baseline, we strictly follow the same hyperparameter search spaces and training protocols as OpenGT, summarized in Appendix Table 5. Our method introduces one additional architectural hyperparameter: the per-head n -hop receptive field. Unless otherwise specified, we fix the number of attention heads to four and search over head hop values $n \in \{1, 3, 6, 12, 24, 48\}$. All experiments are conducted on an NVIDIA GeForce RTX 3090 GPU with 24 GB memory, and all reported results correspond

Table 2: Test accuracy (\uparrow) on node-level benchmark datasets, reported as mean \pm std over 3 runs. “OOM” denotes configurations that resulted in out-of-memory errors for all tested hyperparameter settings. The **best** and second-best results for each dataset are highlighted.

Model	Cora	Citeseer	Pubmed	Chameleon	Squirrel	Actor	Cornell	Texas	Wisconsin
Message Passing Neural Networks									
GCN	0.7180 \pm 0.0298	0.6173 \pm 0.0177	0.7150 \pm 0.0297	0.4415 \pm 0.0169	0.2917 \pm 0.0094	0.2713 \pm 0.0089	0.3243 \pm 0.0441	0.4505 \pm 0.0709	0.4379 \pm 0.0515
GAT	0.7460 \pm 0.0116	0.6123 \pm 0.0162	0.7590 \pm 0.0184	0.4613 \pm 0.0021	0.3016 \pm 0.0086	0.2842 \pm 0.0121	0.3513 \pm 0.0441	0.3604 \pm 0.1469	0.3791 \pm 0.0606
APPNP	0.7713 \pm 0.0101	0.6617 \pm 0.0266	0.7750\pm0.0046	0.4956 \pm 0.0100	0.3333 \pm 0.0088	0.2798 \pm 0.0017	0.4414 \pm 0.0127	0.5405 \pm 0.0000	0.4641 \pm 0.0092
Graph Transformers									
Graphtransformer	0.7913\pm0.0052	0.6717\pm0.0062	0.7420 \pm 0.0099	0.4006 \pm 0.0055	0.2767 \pm 0.0077	0.2873 \pm 0.0006	0.3874 \pm 0.0127	0.6036 \pm 0.0255	0.5229 \pm 0.0462
Graphomer	0.4323 \pm 0.0455	0.4360\pm0.0140	OOM	0.5453 \pm 0.0136	0.4310\pm0.0120	0.3713 \pm 0.0057	0.7117 \pm 0.0127	0.7748 \pm 0.0127	0.7582 \pm 0.0244
SAN	0.5403 \pm 0.0540	OOM	OOM	0.4189 \pm 0.0267	OOM	OOM	0.6667 \pm 0.0337	0.7843 \pm 0.0160	
GPS	0.7150 \pm 0.0051	0.6227 \pm 0.0246	0.7327 \pm 0.0184	0.4905 \pm 0.0092	0.3535 \pm 0.0062	0.3721 \pm 0.0117	0.7297 \pm 0.0221	0.7478 \pm 0.0127	0.7974 \pm 0.0092
DIFFomer	0.7650 \pm 0.0099	0.6447 \pm 0.0217	0.7587 \pm 0.0066	0.4854 \pm 0.0058	0.3602 \pm 0.0070	0.3682 \pm 0.0110	0.6486 \pm 0.0441	0.7207 \pm 0.0337	0.7451 \pm 0.0320
SpecFormer	0.4883 \pm 0.0084	0.4540 \pm 0.0100	0.6973 \pm 0.0079	0.5623\pm0.0089	0.4454\pm0.0141	0.3647 \pm 0.0087	0.7478\pm0.0255	0.7838\pm0.0221	0.7778 \pm 0.0092
Exphomer	0.6120 \pm 0.0213	0.5117 \pm 0.0070	0.6987 \pm 0.0170	0.5161 \pm 0.0068	0.3490 \pm 0.0071	0.3577 \pm 0.0045	0.5405 \pm 0.0441	0.3784 \pm 0.0221	0.6994 \pm 0.0333
GRIT	OOM	OOM	OOM	0.4722 \pm 0.0260	OOM	OOM	0.6486 \pm 0.0584	0.7027 \pm 0.0382	0.8039\pm0.0160
NodeFormer	0.7103 \pm 0.0175	0.5903 \pm 0.0204	0.6953 \pm 0.0144	0.4788 \pm 0.0058	0.3442 \pm 0.0063	0.3520 \pm 0.0047	0.6577 \pm 0.0459	0.6937 \pm 0.0255	0.7386 \pm 0.0403
CoBFormer	0.7243 \pm 0.0118	0.6300 \pm 0.0127	0.7203 \pm 0.0133	0.5124 \pm 0.0057	0.3737 \pm 0.0049	0.3719 \pm 0.0088	0.7117 \pm 0.0337	0.7387 \pm 0.0637	0.7647 \pm 0.0320
SGFormer	0.7703 \pm 0.0021	0.6580 \pm 0.0008	0.7347 \pm 0.0034	0.5080 \pm 0.0010	0.3401 \pm 0.0068	0.3746\pm0.0084	0.7207 \pm 0.0127	0.7568 \pm 0.0221	0.7843 \pm 0.0000
DeGTA	0.7533 \pm 0.0056	0.6190 \pm 0.0232	OOM	0.4920 \pm 0.0045	0.3164 \pm 0.0079	0.3507 \pm 0.0067	0.5315 \pm 0.0459	0.6126 \pm 0.0127	0.5229 \pm 0.0092
Ours (HopFormer)	0.7850\pm0.0125	0.6850\pm0.0346	0.7630\pm0.0122	0.5738\pm0.0278	0.3748 \pm 0.0033	0.3736\pm0.0016	0.7657\pm0.0412	0.7937\pm0.0270	0.8169\pm0.0113

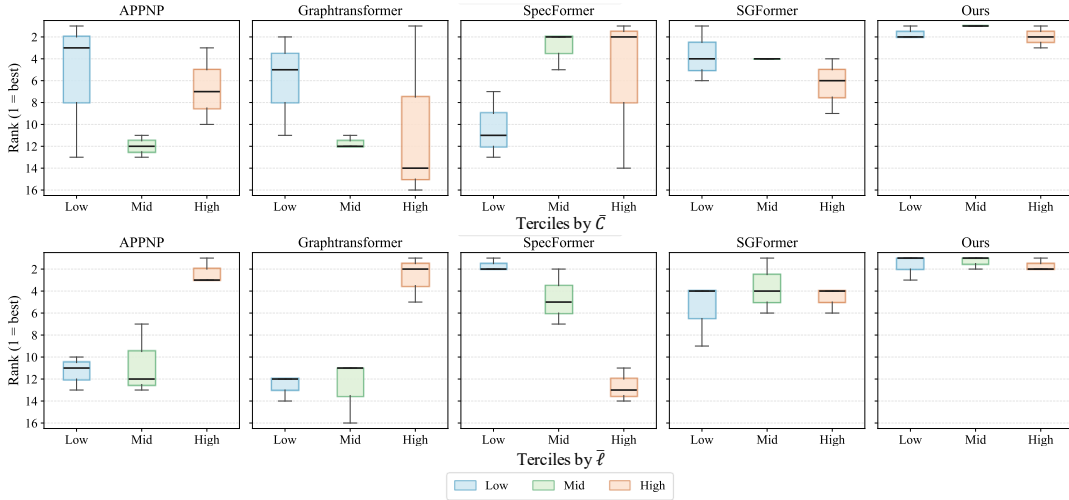


Figure 4: Per-method rank distributions across low, mid, and high terciles of small-world measures: clustering coefficient \bar{C} (top) and average shortest-path length \bar{l} (bottom). Lower ranks indicate better performance. Boxes indicate the interquartile range, center lines denote the median, and whiskers show the data range (excluding outliers).

to the best-performing configuration within this unified search space, ensuring a fair and controlled comparison.

5.2 Experiment Results

We empirically evaluate our approach across a wide range of node-level and graph-level benchmarks to answer three core questions: (i) Is explicit positional or structural encoding necessary for effective graph Transformers? (ii) Is global dense attention always required? (iii) Does the computational complexity of our sparse attention formulation follow the theoretical analysis?

Is Explicit Structural Encoding Necessary? We first examine whether injecting graph structure via explicit positional encodings or architectural modifications is essential for strong performance. [Table 2](#) and [Table 3](#) summarize results on node-

level and graph-level benchmarks, respectively. Across node-level datasets, our method consistently achieves top or near-top performance, outperforming or matching state-of-the-art graph Transformers that rely on sophisticated structural encodings (e.g., Laplacian eigenvectors, random-walk features, or spectral bases). Notably, our approach requires none of these components and instead injects graph structure solely through n -hop mask-guided sparse attention. This demonstrates that explicitly controlling the receptive field via sparsity is sufficient to encode meaningful graph structure, without resorting to complex positional encodings or architectural augmentations. A similar trend holds for graph-level benchmarks in [Table 3](#). Despite its simplicity, our method achieves the best overall performance on OGBG-MolHIV and Peptides-Struct, while remaining competitive on other datasets. These results provide strong empirical evidence that explicit positional or structural encodings are not a prerequisite for effective graph Transformer models.

Table 3: Performance on graph-level benchmark datasets, reported as mean \pm std over 3 runs. “OOM” denotes configurations that resulted in out-of-memory errors for all tested hyperparameter settings. The **best** and second-best results for each dataset are highlighted.

Model	OGBG-MolHIV AUC \uparrow	OGBG-MolPCBA AP \uparrow	Peptides-Func AP \uparrow	Peptides-Struct MAE \downarrow	ZINC MAE \downarrow
Message Passing Neural Networks					
GCN	0.6888 \pm 0.0127	0.0953 \pm 0.0012	0.3614 \pm 0.0036	0.4347 \pm 0.0033	0.6090 \pm 0.0155
GAT	0.7385 \pm 0.0300	0.1012 \pm 0.0015	0.3719 \pm 0.0041	0.4231 \pm 0.0049	0.6225 \pm 0.0096
APPNP	0.7550 \pm 0.0000	0.0973 \pm 0.0011	0.3964 \pm 0.0022	0.4374 \pm 0.0005	0.6619 \pm 0.0067
Graph Transformers					
GraphTransformer	0.6350 \pm 0.0112	0.0968 \pm 0.0001	0.3622 \pm 0.0036	0.4345 \pm 0.0026	0.6038 \pm 0.0151
Graphformer	OOD	OOD	OOD	OOD	0.1305 \pm 0.0072
SAN	OOD	OOD	OOD	OOD	0.1341 \pm 0.0063
GPS	0.7715 \pm 0.0135	OOD	0.6565 \pm 0.0038	0.2512 \pm 0.0008	0.1968 \pm 0.0210
GPS+RWSE	0.7713 \pm 0.0105	0.2888 \pm 0.0019	0.6427 \pm 0.0035	0.2851 \pm 0.0012	0.0681 \pm 0.0004
GPS+GE	OOD	OOD	OOD	OOD	0.1789 \pm 0.0071
DIFFormer	0.7169 \pm 0.0103	0.0785 \pm 0.0021	0.3810 \pm 0.0013	0.4541 \pm 0.0005	0.6602 \pm 0.0294
Exphormer	OOD	OOD	0.4003 \pm 0.0058	0.3297 \pm 0.0085	0.1905 \pm 0.0276
GRIT	0.7608 \pm 0.0165	0.1931 \pm 0.0018	OOD	OOD	0.0607 \pm 0.0000
GraphMLPMixer	0.6889 \pm 0.0146	0.1386 \pm 0.0018	0.4225 \pm 0.0095	0.3065 \pm 0.0019	0.3617 \pm 0.0222
SGFormer	0.6794 \pm 0.0076	0.0933 \pm 0.0040	0.3726 \pm 0.0018	0.4492 \pm 0.0002	0.6703 \pm 0.0033
Ours (HopFormer)	0.7997\pm0.0078	0.1849 \pm 0.0116	0.6467\pm0.0124	0.2503\pm0.0016	0.1306 \pm 0.0194

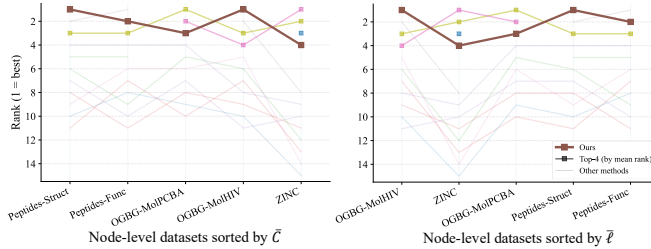


Figure 5: Rank trajectories of different methods across graph-level datasets. In contrast to node-level benchmarks, the top-performing methods exhibit consistently similar ranks, indicating that when small-world effects are weaker, Transformer-based models tend to achieve comparable performance.

Is Global Dense Attention Always Required? We next investigate whether global dense attention is universally beneficial across graphs with different structural properties. To this end, we first analyze the small-world characteristics of each benchmark. Figure 2 visualizes the clustering coefficient \bar{C} and average shortest-path length $\bar{\ell}$ for both node-level and graph-level datasets, where \bar{C} and $\bar{\ell}$ are computed by averaging the per-graph C and ℓ values within each dataset. Node-level benchmarks generally exhibit strong small-world properties, characterized by high clustering and short path lengths, whereas graph-level datasets show substantially weaker small-world effects. We then analyze method behavior across this spectrum. On node-level datasets, where small-world structure is pronounced, rank trajectories in Figure 3 reveal that many existing methods exhibit large performance fluctuations as dataset structure changes. This instability stems from their fixed or implicit receptive fields, which cannot adapt to varying graph connectivity patterns. In contrast, our method maintains consistently strong ranks across all datasets. This effect is further quantified in Figure 4, which groups datasets into low, mid, and high terciles according to \bar{C} and $\bar{\ell}$. Among all methods that achieve rank 1 on at least one benchmark, only our approach exhibits both high median performance and narrow variance across all small-world regimes. This highlights the advantage of explicitly configurable receptive fields. The situation changes for graph-level benchmarks. As shown in Figure 5 and Figure 4,

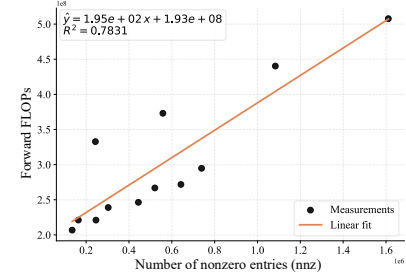


Figure 6: Forward-pass FLOPs as a function of the number of nonzero entries in the n -hop attention masks. Results are obtained on Cornell, Texas, and Wisconsin using single-layer models with different head hop configurations ($\{3, 6, 12, 24\}$, $\{3, 3, 6, 12\}$, $\{3, 3, 3, 6\}$, and $\{3, 3, 3, 3\}$). The linear trend indicates that computation scales proportionally with mask sparsity.

when small-world effects are weak, global attention saturates in effectiveness. The top-performing Transformer-based methods converge to similar ranks, indicating diminishing returns from full global connectivity. These observations collectively suggest that global dense attention is not universally necessary and that the ability to adaptively control the receptive field is critical for generalization across diverse graph structures.

Computational Efficiency and Scalability Finally, we empirically validate our computational complexity analysis. Figure 6 plots forward-pass FLOPs against the number of nonzero entries in the n -hop attention masks across multiple configurations. The results show a clear linear relationship between FLOPs and mask sparsity, confirming that the computational cost of our method scales proportionally with $\text{nnz}(\mathbf{M})$. This validates our theoretical analysis and demonstrates that our approach enables flexible trade-offs between accuracy and efficiency. By adjusting the receptive field according to graph structure, our model can achieve competitive performance with substantially reduced computation when global attention is unnecessary.

6 CONCLUSION

We show that effective graph Transformers do not require explicit positional or structural encodings, nor architectural modifications to the standard Transformer. Injecting topology solely via head-specific n -hop masked sparse attention is sufficient to capture graph structure, while preserving architectural simplicity and providing explicit, interpretable control over receptive fields with a clear efficiency-expressivity trade-off. Across diverse node-level and graph-level benchmarks, this minimal design is competitive with or outperforms prior graph Transformers, and exhibits markedly more stable performance on graphs with strong small-world structure. On graph-level benchmarks where small-world effects are weaker, performance saturates and multiple Transformer variants converge to similar ranks, indicating that dense global attention offers diminishing returns.

Limitations and Future Work. Our analysis of the link between small-world properties and optimal receptive fields remains primarily empirical. A more thorough characterization—ideally with theory—could explain when and why particular

hop budgets are sufficient, and enable automatic selection or learning of n -hop configurations. This would reduce reliance on hyperparameter tuning and improve usability and robustness across new domains and scales.

ACKNOWLEDGEMENTS

This work was supported in part by the DARPA Young Faculty Award, the National Science Foundation (NSF) under Grants #2127780, #2319198, #2321840, #2312517, #2431561, and #2235472, the Semiconductor Research Corporation (SRC), the Office of Naval Research through the Young Investigator Program Award, and Grants #N00014-21-1-2225 and #N00014-22-1-2067, Army Research Office Grant #W911NF2410360. Additionally, support was provided by the Air Force Office of Scientific Research under Award #FA9550-22-1-0253, along with generous gifts from Xilinx and Cisco.

REFERENCES

[1] Chengxuan Ying, Tianle Cai, Shengjie Luo, Shuxin Zheng, Guolin Ke, Di He, Yanming Shen, and Tie-Yan Liu. Do transformers really perform badly for graph representation? *Advances in neural information processing systems*, 34: 28877–28888, 2021.

[2] Devin Kreuzer, Dominique Beaini, Will Hamilton, Vincent Létourneau, and Prudencio Tossou. Rethinking graph transformers with spectral attention. *Advances in Neural Information Processing Systems*, 34:21618–21629, 2021.

[3] Ladislav Rampášek, Michael Galkin, Vijay Prakash Dwivedi, Anh Tuan Luu, Guy Wolf, and Dominique Beaini. Recipe for a general, powerful, scalable graph transformer. *Advances in Neural Information Processing Systems*, 35: 14501–14515, 2022.

[4] Qitian Wu, Wentao Zhao, Zenan Li, David P Wipf, and Junchi Yan. Nodeformer: A scalable graph structure learning transformer for node classification. *Advances in Neural Information Processing Systems*, 2022.

[5] Jinwoo Kim, Dat Nguyen, Seonwoo Min, Sungjun Cho, Moontae Lee, Honglak Lee, and Seunghoon Hong. Pure transformers are powerful graph learners. *Advances in Neural Information Processing Systems*, 35:14582–14595, 2022.

[6] Deyu Bo, Chuan Shi, Lele Wang, and Renjie Liao. Specformer: Spectral graph neural networks meet transformers. In *International Conference on Learning Representations*, 2023.

[7] Qitian Wu, Chenxiao Yang, Wentao Zhao, Yixuan He, David Wipf, and Junchi Yan. Difformer: Scalable (graph) transformers induced by energy constrained diffusion. *International Conference on Learning Representations*, 2023.

[8] Hamed Shirzad, Ameya Velingker, Balaji Venkatachalam, Danica J Sutherland, and Ali Kemal Sinop. Exphormer: Sparse transformers for graphs. In *International Conference on Machine Learning*, pages 31613–31632. PMLR, 2023.

[9] Liheng Ma, Chen Lin, Derek Lim, Adriana Romero-Soriano, Puneet K Dokania, Mark Coates, Philip Torr, and Ser-Nam Lim. Graph inductive biases in transformers without message passing. In *International Conference on Machine Learning*, pages 23321–23337. PMLR, 2023.

[10] David Buterez, Jon Paul Janet, Dino Oglic, and Pietro Liò. An end-to-end attention-based approach for learning on graphs. *Nature Communications*, 16(1):5244, 2025.

[11] Ashish Vaswani, Noam Shazeer, Niki Parmar, Jakob Uszkoreit, Llion Jones, Aidan N Gomez, Łukasz Kaiser, and Illia Polosukhin. Attention is all you need. *Advances in neural information processing systems*, 30, 2017.

[12] Tom Brown, Benjamin Mann, Nick Ryder, Melanie Subbiah, Jared D Kaplan, Prafulla Dhariwal, Arvind Neelakantan, Pranav Shyam, Girish Sastry, Amanda Askell, et al. Language models are few-shot learners. *Advances in neural information processing systems*, 33:1877–1901, 2020.

[13] Anurag Arnab, Mostafa Dehghani, Georg Heigold, Chen Sun, Mario Lučić, and Cordelia Schmid. Vivit: A video vision transformer. In *Proceedings of the IEEE/CVF international conference on computer vision*, pages 6836–6846, 2021.

[14] Justin Gilmer, Samuel S Schoenholz, Patrick F Riley, Oriol Vinyals, and George E Dahl. Neural message passing for quantum chemistry. In *International conference on machine learning*, pages 1263–1272. Pmlr, 2017.

[15] Kenta Oono and Taiji Suzuki. Graph neural networks exponentially lose expressive power for node classification. In *International Conference on Learning Representations*, 2020.

[16] Jake Topping, Francesco Di Giovanni, Benjamin Paul Chamberlain, Xiaowen Dong, and Michael M Bronstein. Understanding over-squashing and bottlenecks on graphs via curvature. In *International Conference on Learning Representations*, 2022.

[17] Nicolas Keriven and Gabriel Peyré. Universal invariant and equivariant graph neural networks. *Advances in neural information processing systems*, 32, 2019.

[18] Ziniu Hu, Yuxiao Dong, Kuansan Wang, and Yizhou Sun. Heterogeneous graph transformer. In *Proceedings of the web conference 2020*, pages 2704–2710, 2020.

[19] Jiawei Zhang, Haopeng Zhang, Congying Xia, and Li Sun. Graph-bert: Only attention is needed for learning graph representations. *arXiv preprint arXiv:2001.05140*, 2020.

[20] Adi Haviv, Ori Ram, Ofir Press, Peter Izsak, and Omer Levy. Transformer language models without positional encodings still learn positional information. *arXiv preprint arXiv:2203.16634*, 2022.

[21] Chuanyang Zheng, Yihang Gao, Han Shi, Minbin Huang, Jingyao Li, Jing Xiong, Xiaozhe Ren, Michael Ng, Xin Jiang, Zhenguo Li, et al. Dape: Data-adaptive positional encoding for length extrapolation. *Advances in Neural Information Processing Systems*, 37:26659–26700, 2024.

[22] Jie Wang, Tao Ji, Yuanbin Wu, Hang Yan, Tao Gui, Qi Zhang, Xuan-Jing Huang, and Xiaoling Wang. Length generalization of causal transformers without position encoding. In *Findings of the Association for Computational Linguistics: ACL 2024*, pages 14024–14040, 2024.

[23] Amirhossein Kazemnejad, Inkit Padhi, Karthikeyan Nateyan Ramamurthy, Payel Das, and Siva Reddy. The impact of positional encoding on length generalization in transformers. *Advances in Neural Information Processing Systems*, 2023.

[24] Duncan J Watts and Steven H Strogatz. Collective dynamics of ‘small-world’ networks. *nature*, 393(6684):440–442, 1998.

[25] Ari Zitin, Alexander Gorowara, Shane Squires, Mark Herrera, Thomas M Antonsen, Michelle Girvan, and Edward Ott. Spatially embedded growing small-world networks. *Scientific reports*, 4(1):7047, 2014.

[26] Matt Deitke, Christopher Clark, Sangho Lee, Rohun Tripathi, Yue Yang, Jae Sung Park, Mohammadreza Salehi, Niklas Muennighoff, Kyle Lo, Luca Soldaini, et al. Molmo and pixmo: Open weights and open data for state-of-the-art vision-language models. In *Proceedings of the Computer Vision and Pattern Recognition Conference*, pages 91–104, 2025.

[27] Chengyue Wu, Xiaokang Chen, Zhiyu Wu, Yiyang Ma, Xingchao Liu, Zizheng Pan, Wen Liu, Zhenda Xie, Xingkai Yu, Chong Ruan, et al. Janus: Decoupling visual encoding for unified multimodal understanding and generation. In *Proceedings of the Computer Vision and Pattern Recognition Conference*, 2025.

[28] Carl Yang, Aydin Buluç, and John D Owens. Design principles for sparse matrix multiplication on the gpu. In *European Conference on Parallel Processing*. Springer, 2018.

[29] Bo Jiang, Ziyan Zhang, Doudou Lin, Jin Tang, and Bin Luo. Semi-supervised learning with graph learning-convolutional networks. In *Proceedings of the IEEE/CVF conference on computer vision and pattern recognition*, 2019.

[30] Chulhee Yun, Srinadh Bhojanapalli, Ankit Singh Rawat, Sashank J Reddi, and Sanjiv Kumar. Are transformers universal approximators of sequence-to-sequence functions? In *International Conference on Learning Representations*, 2020.

[31] Jean-Baptiste Cordonnier, Andreas Loukas, and Martin Jaggi. On the relationship between self-attention and convolutional layers. In *International Conference on Learning Representations*, 2020.

[32] Jiachen Tang, Zhonghao Wang, Sirui Chen, Sheng Zhou, Jiawei Chen, and Jiajun Bu. Opengt: A comprehensive benchmark for graph transformers. *arXiv preprint arXiv:2506.04765*, 2025.

[33] Qitian Wu, Wentao Zhao, Chenxiao Yang, Hengrui Zhang, Fan Nie, Haitian Jiang, Yatao Bian, and Junchi Yan. SgFormer: Simplifying and empowering transformers for large-graph representations. *Advances in Neural Information Processing Systems*, 2023.

[34] Vijay Prakash Dwivedi and Xavier Bresson. A generalization of transformer networks to graphs. *arXiv preprint arXiv:2012.09699*, 2020.

[35] Xiaoxin He, Bryan Hooi, Thomas Laurent, Adam Perold, Yann LeCun, and Xavier Bresson. A generalization of vit/mlp-mixer to graphs. In *International conference on machine learning*. PMLR, 2023.

[36] Yujie Xing, Xiao Wang, Yibo Li, Hai Huang, and Chuan Shi. Less is more: on the over-globalizing problem in graph transformers. In *International Conference on Learning Representations*, 2024.

[37] Xiaotang Wang, Yun Zhu, Haizhou Shi, Yongchao Liu, and Chuntao Hong. Graph triple attention networks: A decoupled perspective. In *Proceedings of the 31st ACM SIGKDD Conference on Knowledge Discovery and Data Mining V. 1*, 2025.

[38] TN Kipf. Semi-supervised classification with graph convolutional networks. *arXiv preprint arXiv:1609.02907*, 2016.

[39] Petar Veličković, Guillem Cucurull, Arantxa Casanova, Adriana Romero, Pietro Lio, and Yoshua Bengio. Graph attention networks. In *International Conference on Learning Representations*, 2018.

[40] Johannes Gasteiger, Aleksandar Bojchevski, and Stephan Günnemann. Predict then propagate: Graph neural networks meet personalized pagerank. In *International Conference on Learning Representations*, 2019.

[41] Prithviraj Sen, Galileo Namata, Mustafa Bilgic, Lise Getoor, Brian Galligher, and Tina Eliassi-Rad. Collective classification in network data. *AI magazine*, 29(3):93–93, 2008.

[42] Benedek Rozemberczki, Ryan Davies, Rik Sarkar, and Charles Sutton. Gemsec: Graph embedding with self clustering. In *Proceedings of the 2019 IEEE/ACM international conference on advances in social networks analysis and mining*, 2019.

[43] Oleksandr Shchur, Maximilian Mumme, Aleksandar Bojchevski, and Stephan Günnemann. Pitfalls of graph neural network evaluation. *arXiv preprint arXiv:1811.05868*, 2018.

[44] Hongbin Pei, Bingzhe Wei, Kevin Chen-Chuan Chang, Yu Lei, and Bo Yang. Geom-gcn: Geometric graph convolutional networks. *arXiv preprint arXiv:2002.05287*, 2020.

[45] John J Irwin, Teague Sterling, Michael M Mysinger, Erin S Bolstad, and Ryan G Coleman. Zinc: a free tool to discover chemistry for biology. *Journal of chemical information and modeling*, 52(7):1757–1768, 2012.

[46] Weihua Hu, Matthias Fey, Marinka Zitnik, Yuxiao Dong, Hongyu Ren, Bowen Liu, Michele Catasta, and Jure Leskovec. Open graph benchmark: Datasets for machine learning on graphs. *Advances in neural information processing systems*, 2020.

[47] Vijay Prakash Dwivedi, Ladislav Rampášek, Michael Galkin, Ali Parviz, Guy Wolf, Anh Tuan Luu, and Dominique Beaini. Long range graph benchmark. *Advances in Neural Information Processing Systems*, 2022.

APPENDIX

7 ADDITIONAL RELATED WORK AND BACKGROUND

Graph Transformers. Graph Transformers extend self-attention to graph-structured data by treating nodes—and in some cases edges—as tokens, while injecting structural information to compensate for the lack of canonical ordering. Most existing approaches encode graph structure through explicit positional or structural encodings, including shortest-path-distance and degree biases in Graphomer [1], Laplacian eigenvectors or spectral features [34, 2, 19], or hybrid Transformer–MPNN architectures such as GraphGPS and GRIT that combine global attention with message passing [3, 9]. While empirically effective, these methods introduce encoding-dependent inductive biases and typically retain dense global self-attention, resulting in quadratic or higher complexity that is misaligned with graph sparsity. Distance-restricted or sparse attention variants have been explored [1, 2], but are usually tied to fixed encodings or applied as secondary constraints, without explicit, per-head control over receptive fields. In contrast, our approach injects graph structure solely through head-specific n -hop attention masks, enabling topology-aligned sparse attention with interpretable receptive fields, while preserving the standard Transformer architecture without positional encodings or auxiliary modules.

8 PROOFS

8.1 Proof of Theorem 1

Proof. Let $\mathbf{M}^{(h)} \in \{0, 1\}^{(N+M) \times (N+M)}$ denote the head-specific attention mask defined in Equation 6. By construction, $\mathbf{M}_{ij}^{(h)} = 1$ if and only if token j is reachable from token i within at most n_h hops in \tilde{G} .

Under the masked attention formulation in Equation 7, attention scores are computed only on the support of $\mathbf{M}^{(h)}$. That is, for any j such that $\mathbf{M}_{ij}^{(h)} = 0$, the corresponding query–key interaction is excluded from the softmax normalization, yielding an effective attention weight $\alpha_{ij}^{(h)} = 0$.

Consequently, the output of head h at token i can be written as

$$\mathbf{z}_i^{(h)} = \sum_{j: \mathbf{M}_{ij}^{(h)}=1} \alpha_{ij}^{(h)} \mathbf{W}_V^{(h)} \mathbf{h}_j^{(0)} = \sum_{j \in \mathcal{N}_{n_h}(i)} \alpha_{ij}^{(h)} \mathbf{W}_V^{(h)} \mathbf{h}_j^{(0)},$$

where $\mathcal{N}_{n_h}(i)$ denotes the n_h -hop neighborhood of i in \tilde{G} . Therefore, the representation $\mathbf{z}_i^{(h)}$ depends only on tokens within this neighborhood, completing the proof. \square

8.2 Proof of Theorem 2

Proof. Consider two tokens i and j such that $j \in \mathcal{N}_{n_{h'}}(i)$ but $j \notin \mathcal{N}_{n_h}(i)$ for some $h \neq h'$. By Theorem 1, head h' can incorporate information from j into $\mathbf{z}_i^{(h')}$, whereas head h cannot.

Let $\mathbf{z}_i = [\mathbf{z}_i^{(1)}; \dots; \mathbf{z}_i^{(H)}]$ denote the concatenated multi-head output. Then \mathbf{z}_i jointly encodes information from multiple, distinct neighborhood scales. No single-hop-budget head can replicate this representation: a smaller hop budget excludes j , while a larger hop budget necessarily aggregates additional nodes beyond $\mathcal{N}_{n_h}(i)$, yielding a different function.

By Assumptions 1 and 2, these differences are preserved through value projections and post-attention mappings. Hence, the function class realizable by multi- n -hop heads strictly contains that of uniform-hop heads. \square

9 ADDITIONAL TABLES

Table 4: Statistics of the datasets used in the benchmark.

Dataset	Level	#Graphs	Avg. Nodes	Avg. Edges	#Classes	#Features	Metric
Cora	Node	1	2,708	5,429	7	1,433	Accuracy
Citeseer	Node	1	3,327	4,732	6	3,703	Accuracy
Pubmed	Node	1	19,717	44,338	3	500	Accuracy
Squirrel	Node	1	5,201	217,073	10	2,089	Accuracy
Chameleon	Node	1	2,277	31,421	10	2,325	Accuracy
Actor	Node	1	7,600	30,019	5	931	Accuracy
Texas	Node	1	183	325	5	1,703	Accuracy
Cornell	Node	1	183	298	5	1,703	Accuracy
Wisconsin	Node	1	251	515	5	1,703	Accuracy
ZINC	Graph	12,000	23.2	49.8	—	28	MAE
OGBG-MolHIV	Graph	41,127	25.5	27.5	2	9	ROC-AUC
OGBG-MolPCBA	Graph	437,929	26.0	28.1	128	9	AP
Peptides-Func	Graph	15,535	151	307	10	9	AP
Peptides-Struct	Graph	15,535	151	307	11	9	MAE

Table 5: Hyperparameter search space for all implemented Graph Transformer models.

Algorithm	Hyperparameter Search Space
General Settings	
Learning rate	$\{10^{-4}, 3 \times 10^{-4}, 10^{-3}, 3 \times 10^{-3}, 10^{-2}\}$
Weight decay	$\{10^{-5}, 3 \times 10^{-5}, 10^{-4}, 3 \times 10^{-4}, 10^{-3}\}$
Number of layers	$\{1, 2, 3, 4\}$
Number of attention heads	$\{1, 2, 3, 4\}$
Dropout	$\{0, 0.2, 0.5, 0.8\}$
Attention dropout	$\{0, 0.2, 0.5, 0.8\}$
SGFormer [33]	Aggregate method: {add, cat} Graph weight: {0.2, 0.5, 0.8}
DIFFFormer [7]	Graph weight: {0.2, 0.5, 0.8}
DeGTA [37]	$K: \{2, 4, 8\}$
Ours	Attention head configuration: fixed to 4 heads; each head hop $n \in \{1, 3, 6, 12, 24, 48\}$